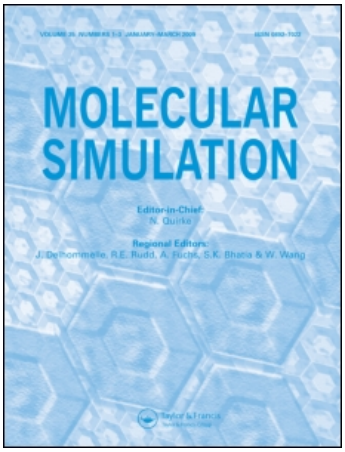

Molecular Simulation

Publication details, including instructions for authors and subscription information:
http://www.informaworld.com/smpp/title~content=t713644482

Theoretical Study On The Reaction Mechanism Of $Gecl_3ch_2ch_2cooh+h_2gecl_2ohch_2ch_2cooh+hcl$

Y. Z. Fang[a]; W. Y. Ma[a]; J. Zhang[a]; J. H. Zhou[a]; C. Lu[a]
[a] Department of Chemical Engineering, Shandong Institute of Light Industry, Jinan, P.R. China

To cite this Article Fang, Y. Z. , Ma, W. Y. , Zhang, J. , Zhou, J. H. and Lu, C.(2008) 'Theoretical Study On The Reaction Mechanism Of $Gecl_3ch_2ch_2cooh+h_2gecl_2ohch_2ch_2cooh+hcl$', Molecular Simulation, 34: 5, 533 — 540
To link to this Article: DOI: 10.1080/08927020701829872
URL: http://dx.doi.org/10.1080/08927020701829872

Molecular Simulation
Vol. 34, No. 5, April 2008, 533–540

Taylor & Francis
Taylor & Francis Group

Theoretical study on the reaction mechanism of $GeCl_3CH_2CH_2COOH + H_2O \rightarrow GeCl_2OHCH_2CH_2COOH + HCl$

Y.Z. Fang, W.Y. Ma*, J. Zhang, J.H. Zhou and C. Lu

Department of Chemical Engineering, Shandong Institute of Light Industry, Jinan, P.R. China

(Received 9 July 2007; final version received 24 November 2007)

The mechanism and dynamical properties for the title reaction have been investigated theoretically. Three reaction pathways have been found. Geometries, vibrational frequencies, infra-red (IR) intensities and relative energies for various stationary points in the three reaction channels have been determined respectively. The corresponding rate constants at the B3LYP/6-31++G(2d,2p) level have been deduced over a wide temperature range of 200–2000 K by using canonical variational transition state theory with small curvature tunnelling effect. Solvent effects are taken into account via the Onsager model of self-constant reaction field at the same level of theory. This preliminary study shows that the complex formation is favoured by the use of water solvent.

Keywords: 3-trichlorogermyl-propanoic acid; hydrolysation reation; DFT; canonical variational transition state theory; solvent effect

1. Introduction

Organic germanium compounds exhibit excellent characteristics as biological response modifiers [1]. For example, they are active in inducing interferon; they can activate macrophage or Natural killer (NK) cells and have antitumour activities based thereon. In addition, since these compounds exhibit desirable pharmaceutical activities, such as abilities to control enkephalin-degrading enzymes, to improve Ca metabolism, and to have a low level of toxicity, it is thought that they can be employed as useful pharmaceuticals.

In recent years, there has been a growing interest [2–5] in the organic germanium for its biologic activity. For instance, organic germanium has been used clinically in many parts of the world to treat a wide spectrum of illnesses, especially the known organogermanium compound of carboxyethylgermanium sesquioxide and generally called Ge-132 [6] synthesised by Asai's group in 1967, which now has attracted the attention of many researchers. This synthesised organogermanium compound with immunomodulaing activities was shown to be an inducer of anti-suppressor T cells in normal mice [7]. The syntheses, characterisation and properties of a series of organogermanium structures (cyclic or linear) containing selenium, with similar structure to Ge-132, have been reported [8]. Along with the increasing interest of Ge-132, the elucidation of its synthetic mechanism has received more attention; however, no theoretical study has yet been found.

We have initiated a systematic and theoretical study of the application of *ab initio* electronic calculations combined with the variational transition state (TS) theory for the reactions of Ge-132. The synthesis of Ge-132 proceeds via two steps: the addition reaction and the hydrolysation reaction. The step of addition reaction has been examined in our previous study. Our objective in embarking on the present work was to make a systematic theoretical survey of the hydrolysed reaction mechanism of 3-(trichlorogermyl) propanoic acid. This work is now completed by quantum chemical calculations. Geometries, energies, vibrational frequencies of reactants, products and TSs are obtained, and the theoretical rate constants are also calculated, and we hope these results will be valuable for better understanding the reaction mechanism of the Ge-132 system and the synthesis of Ge-132 derivatives.

2. Computational methods

It is a well-known fact that the density functional theory (DFT) methods achieve significantly greater accuracy than Hartree–Fock theory at only a modest increase in cost, and at a cost far less than Moller-plesset (MP2) for medium-size and larger molecular systems. They do so by including some of effects of electron correlation much less expensively than traditional correlated methods. The hybrid B3LYP [9,10] method of DFT has proven to be superior to the traditional functionals defined

*Corresponding author. Email: mawy@sdili.edu.cn

ISSN 0892-7022 print/ISSN 1029-0435 online

DOI: 10.1080/08927020701829872
http://www.informaworld.com

so far. Therefore we selected the B3LYP as the leading method in our investigation. But B3LYP without diffuse functions is inadequate, for such a computing system containing chlorin atom, and for germanium one probably also needs two d functions. So we chose a basis as large as the 6-31++G(2d,2p) which includes polarisation and diffuse functions on both hydrogen and larger atoms, and this was also used for the energy calculations in solution in order to include long-range interactions as efficiently as possible.

The geometries of reactants, TSs, and products were fully optimised at HF/6-31G(d), B3LYP/6-31G(d, p), and B3LYP/6-31++G(2d,2p) levels. The corresponding harmonic vibrational frequencies were calculated at the same level in order to verify whether the stationary points were local minima or saddle points. The TSs were verified to connect with the designated reactants and products by performing intrinsic reaction coordinate (IRC) analysis. At B3LYP/6-31++G(2d,2p) level, the minimum energy paths (MEP) have been obtained with a gradient step size of $0.02\,\text{amu}^{1/2}$ bohr in mass-weighted Cartesian coordinates. The force constant matrices of the stationary points and selected nonstationary points near the TSs along the MEP have been also calculated in order to do the following kinetics calculations. The single-point energy calculations for all stationary points and the selected points along the MEPs were performed at B3LYP/6-31++G(2d,2p) level. The initial optimised geometry for the complexes were processed without the solvent effects. In a further step, using the self-constant reaction field (SCRF)-Onsager model [11], the optimisations were again performed to determinate the subject properties of the stationary points along the MEP in solution media at the same level. All the calculations above were performed by using the Gaussian 03 program suite [12], and parts of them were carried out in Virtual Laboratory of Computational Chemistry, Computer NetWork Information Center, Chinese Academy of Sciences. Electronic structural information was further used to compute the theoretical rate constants. The rate constants and activation energies at various temperatures were calculated by using the conventional TS theory (TST) and canonical variational TST (CVT) in the Polyrate 9.0 program [13]. The CVT was based on varying the dividing surface along a reference path to minimise the rate constant. Furthermore, the CVT rate constants were corrected with the small curvature tunnelling (SCT) transmission coefficient.

3. Results and discussion

3.1 Optimised geometries and frequencies

Geometric parameters for the part of reactants, products, and the TSs in gas phase optimised at B3LYP/6-31++G(2d,2p) level are displayed in Figure 1. In order to facilitate the discussion, each stationary point in this figure is labelled with a number. While the minima are associated with numbers from 1a to 3a, the TSs connecting two minima X and Y are defined by TSX/Y.

In Figure 1, there are two isomers [2a,3a] of optimised geometry for the equilibrium conformation of $GeCl_2OHCH_2CH_2COOH$, and three TSs [TS1/2a, TS1/2b, TS1/3] for the title reaction. At B3LYP/6-31++G(2d,2p) level, between the two isomers, 2a is slightly lower in energy than 3a, and the order of kinetic stability of these three TSs is TS1/2b < TS1/2a < TS1/3 (Table 1). TS1/2b is 4.5 and 40.2 kJ/mol lower in energy than TS1/2a and TS1/3, respectively. Table 1 shows energies at different levels and relative energies at B3LYP/6-31++G(2d,2p) level of various species in the reactions. It has been shown that it is important to use large basis sets to obtain accurate energies, so we selected B3LYP/6-31++G(2d,2p) level as the leading method in our calculations.

Frequency calculations are carried out for all reactants, products, and TSs. Zero-point energies and part of vibrational frequencies are listed in Table 2. In the IR spectra of $GeCl_3CH_2CH_2COOH$, the $427.5\,\text{cm}^{-1}$ of Ge—Cl stretch is in agreement with the available experimental values of $400\,\text{cm}^{-1}$. The modes corresponding to the IR peaks of 1a, 2a and 3a with carbonyl stretch, used to identify the C═O double bond, seem to overestimate the higher frequencies; however, our scaled frequencies are in reasonable agreement with the experimental value of $1746\,\text{cm}^{-1}$. For TSs, the character of the stationary points is confirmed by normal-mode analysis, which yields one and only one imaginary frequency (Table 2) whose eigenvector corresponds to the direction of the reaction. On the other hand, all the optimised stable structures have positive frequencies.

3.2 Pathway

In order to confirm the reaction mechanism and characterise the nature of the TSs, the IRC calculations were performed using the B3LYP/6-31++G(2d,2p) method. The title reaction involves three possible reaction pathways: 1a + 1b → TS1/2a → 2a + 2b, 1a + 1b → TS1/2b → 2a + 2b, 1a + 1b → TS1/3 → 3a + 2b, respectively. Vibrational analysis and IRC calculations indicate that both TS1/2a and TS1/2b connect the reactants of 1a + 1b and the products of 2a + 2b, and TS1/3 connects the reactants of 1a + 1b and the products of 3a + 2b. The overall profile of the potential energy surface is presented in Figure 2. TSs of TS1/2a and TS1/2b, for the reaction of 1a + 1b → 2a + 2b, were located. At B3LYP/6-31+ +G(2d,2p) level the negative

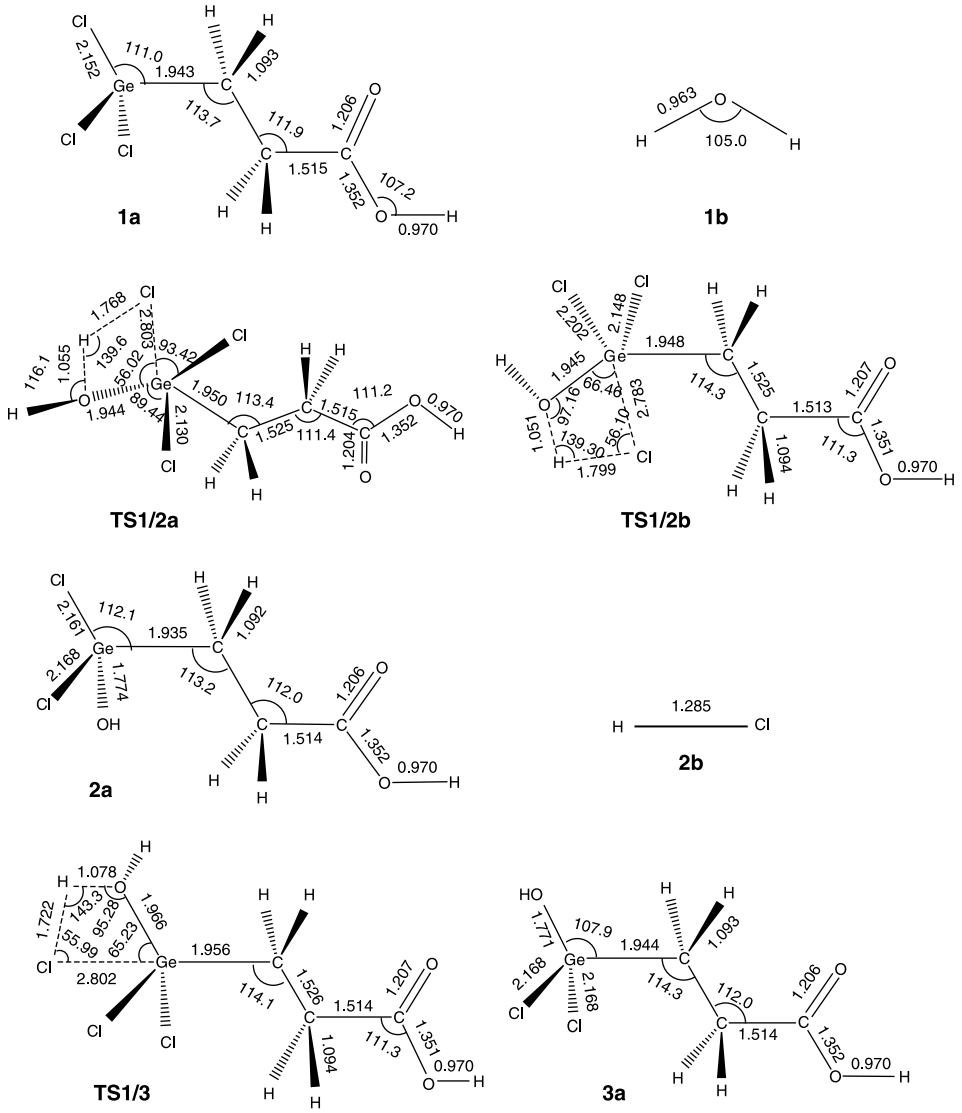

Figure 1. The optimised B3LYP/6-31 + +G(2d,2p) geometrical parameters for the stationary points on the potential energy surface. The distances are in angstroms, the angles are in degrees.

eigenvalue of the Hessian matrix corresponds to imaginary frequencies of 155.4i cm^{-1} and 146.8i cm^{-1}, respectively. With analysis of the normal mode associated with the imaginary frequency, it is clear that the largest displacements are for H in 1b and Cl in 1a, which move together to form the new H—Cl bond. We also obtained the TS of TS1/3 for the reaction of 1a + 1b → 3a + 2b.

The changes of the bond lengths along the three reaction pathways are plotted in Figure 3. From Figure 3, we can see that the distances of the bond Ge—Cl and H—O, which will be broken, increase by 30.24%, 29.34%, 30.22% and 9.60%, 9.18%, 12.02% with respect to the equilibrium bond distances of 1a and 1b; The distances of Ge—O and H—Cl, which will be formed, are 1.0957, 1.0961, 1.1105 and 1.3905, 1.4002, 1.3400 times, respectively, as large as the equilibrium bond distances in the molecule of 2a and 2b.

3.3 Rate constants

The CVT with a SCT effect correction, which has been successfully performed for several reactions [14–17], is an effective method to calculate the rate constants. In this paper, we have used this method to study the title reaction over a wide temperature range 200–2000 K. In order to calculate the rate constants, 30 points near the TSs along the MEP were selected, and we have chosen the energies computed at the B3LYP/6-31 + +G(2d,2p) level.

Table 1. Energies (E) and relative energies (E_{rel}) of various species in the title reaction at different levels.

Species	E (a.u.) HF/6-31G(d)	B3LYP/6-31G(d,p)	B3LYP/6-31++G(2d,2p)	E_{rel} kJ mol^{-1}
1a + 1b	−3794.1285	−3799.9489	−3800.2281	0
TS1/3	−3794.0752	−3799.9196	−3800.1855	111.9259
TS1/2b	−3794.9393	−3799.9343	−3800.1991	76.2541
TS1/2a	−3794.0954	−3799.9357	−3800.2008	71.7256
2a + 2b	−3794.1228	−3799.9466	−3800.2192	23.6071
3a + 2b	−3794.123	−3799.9468	−3800.2191	23.7216

Table 2. Harmonic vibrational frequencies and zero-point energies at B3LYP/6-311G (d, p) level.

Species	Vibrational frequencies (cm^{-1}) and IR intensity (km/mol) (in parentheses)							ZPE (kJ mol^{-1})
H_2O	1627.4	3925.6	3814.3					56.0283834
(1b)	(78.3)	(56.5)	(6.1)					
$GeCl_3CH_2CH_2COOH$	1813.5	1144.5	427.5	3756.4	420.6	1401.3	1218.6	223.39151835
(1a)	(282.3)	(233.9)	(96.4)	(81.1)	(81.0)	(73.5)	(73.1)	
TS1/3	−215.2	2020.1	1017.9	1809.9	1144.4	766.2	1363.8	282.01128012
	(31.8)	(873.2)	(483.4)	(286.7)	(274.8)	(166.9)	(260.1)	
TS1/2a	−155.4	2328.3	1814.5	1341	1144.5	432.6	745.2	284.43725136
	(25.6)	(897.6)	(282.3)	(244.9)	(235.3)	(151.1)	(184.9)	
TS1/2b	−146.8	2382.4	1032.9	1809.5	1371.5	428.6	769.2	285.08312682
	(27.3)	(873.2)	(300.7)	(282.8)	(263.6)	(211.5)	(172.4)	
HCl	2924.1							17.49114762
(2b)	(36.1)							
$GeCl_2OHCH_2CH_2COOH$	1813.0	1144.3	418.9	733.3	3856.9	3735.0	1223.4	255.9236241
(2a)	(282.9)	(232.1)	(115.4)	(91.4)	(89.0)	(76.8)	(70.8)	
$GeCl_2OHCH_2CH_2COOH^2$	1813.6	1144.4	411.9	3857.2	733.9	243.3	1222.6	255.88483011
(3a)	(287.3)	(233.0)	(100.3)	(92.8)	(91.8)	(87.7)	(72.5)	

The classical potential energy (V_{MEP}), ground-state vibrationally adiabatic energy (V_a^G), and zero-point energy as functions of s (amu)$^{1/2}$ bohr are plotted in Figure 4. In Figure 4(b), the curves V_a^G look slightly different from the curves V_{MEP} in shape, which implies that the variational effect may be significant on the calculations of the rate constants of the reaction channels 1a + 1b → TS1/2b → 2a + 2b. In Figure 4(a) and 4(c), the shapes of the curve V_a^G and V_{MEP} are very similar to the reaction channel 1a + 1b → TS1/2a → 2a + 2b and 1a + 1b → TS1/3 → 3a + 2b, which implies that the variational effect on the calculations of the rate constants is not significant.

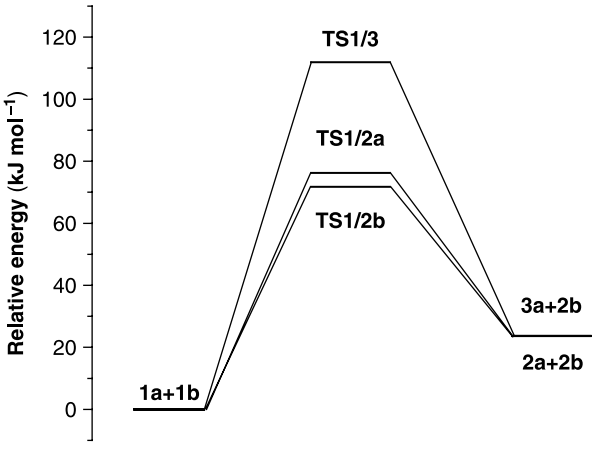

Figure 2. Overall profile of the potential energy surface for title reaction obtained in B3LYP/6-31++G(2d,2p) calculations (dotted line connects stationary points for the whole state).

Calculated rate constants for the three reaction channels are summarised in Table 3. As shown in Table 3, the CVT and CVT/SCT rate constants are close to each other in the lower temperature range, and deviate substantially in the higher temperature range. The total rate constant is obtained from the sum of the individual rate constants associated with the three reaction channels. The corresponding Arrhenius plots for the theoretical rate constants and the temperature dependence of the $k1/k$, $k2/k$ and $k3/k$ branching ratios are shown in Figure 5. In Figure 5(b), the theoretical branching ratios of $k2/k$ are about 0.607–0.879 in the temperature region 300–2000 K, which suggest that the title reaction proceeds predominantly via 1a + 1b → TS1/2b → 2a + 2b over the whole temperature range, and that the contribution of 1a + 1b → TS1/2a → 2a + 2b to the total rate constant is considerably less.

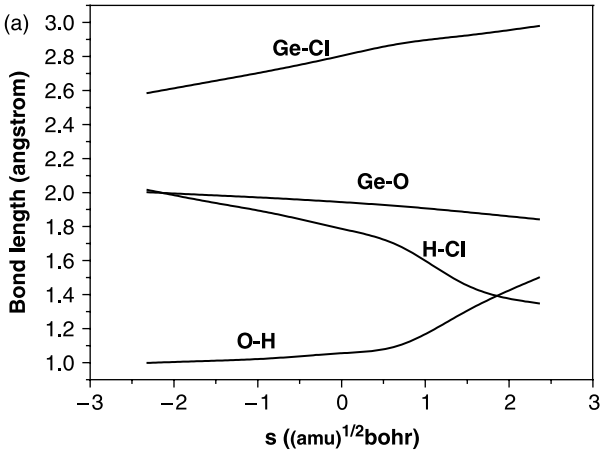

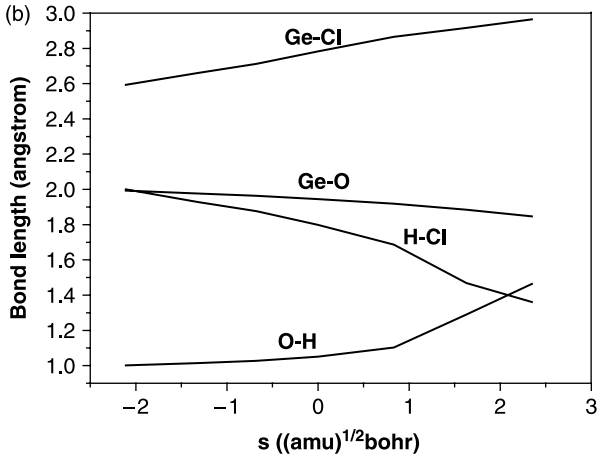

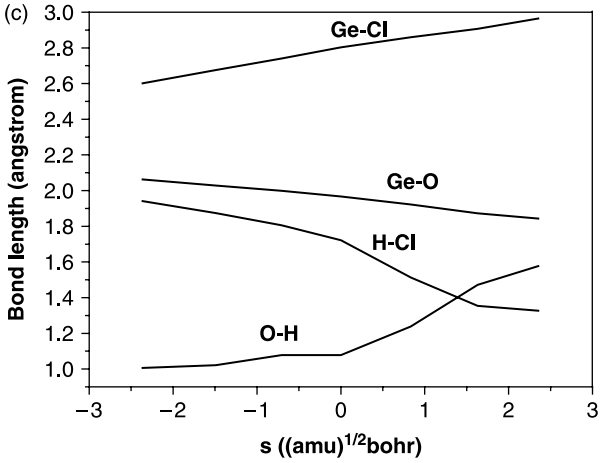

Figure 3. Changes of the bond lengths along the three reaction channels plotted vs. the reaction coordinate at the B3LYP/6-31 + +G(2d,2p) level. The transition state is at $S = 0$. (a) The 1a + 1b → TS1/2a → 2a + 2b reaction channel; (b) the 1a + 1b → TS1/2b → 2a + 2b reaction channel; (c) the 1a + 1b → TS1/3 → 3a + 2b reaction channel.

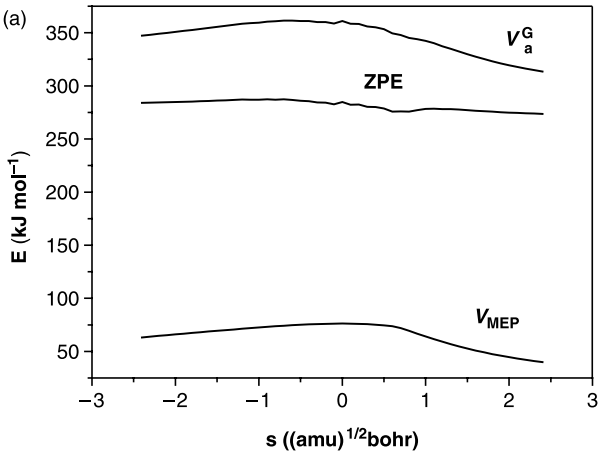

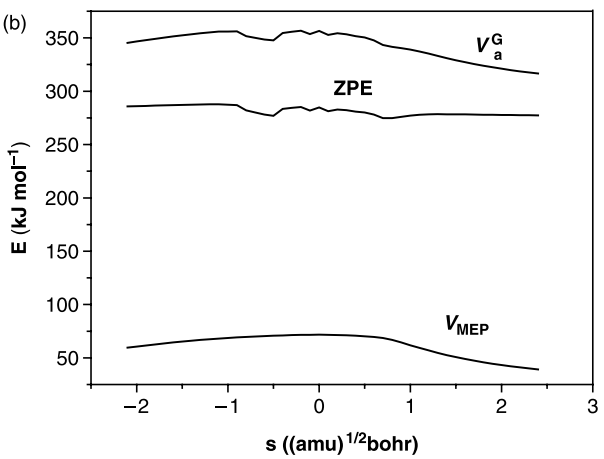

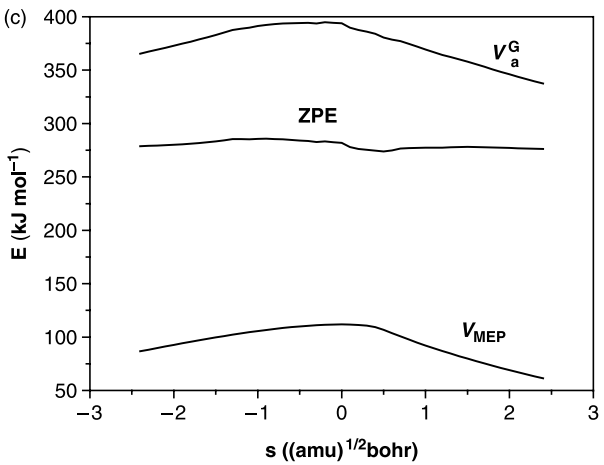

Figure 4. Classical potential energy curve (V_{MEP}), ground-state vibrationally adiabatic energy curve (V_a^G), and zero-point energy curve (ZPE) as functions of s (amu)$^{1/2}$ bohr at the B3LYP/6-31 + +G(2d,2p) level. (a) The 1a + 1b → TS1/2a → 2a + 2b reaction channel; (b) the 1a + 1b → TS1/2b → 2a + 2b reaction channel; (c) the 1a + 1b → TS1/3 → 3a + 2b reaction channel.

Table 3. Calculated forward rate constants (in $cm^3\,molecule^{-1}\,s^{-1}$) for the three reaction channels.

	1a + 1b → TS1/2a → 2a + 2b		1a + 1b → TS1/2b → 2a + 2b		1a + 1b → TS1/3 → 2a + 2b	
T(K)	CVT	CVT/SCT	CVT	CVT/SCT	CVT	CVT/SCT
200	1.66×10^{-36}	1.69×10^{-36}	2.98×10^{-35}	3.13×10^{-35}	4.99×10^{-45}	5.17×10^{-45}
300	1.76×10^{-29}	1.77×10^{-29}	1.26×10^{-28}	1.28×10^{-28}	4.44×10^{-35}	4.49×10^{-35}
350	1.85×10^{-27}	1.51×10^{-27}	1.10×10^{-26}	1.01×10^{-26}	3.21×10^{-32}	3.23×10^{-32}
400	6.01×10^{-26}	5.04×10^{-26}	2.99×10^{-25}	2.77×10^{-25}	4.59×10^{-30}	4.61×10^{-30}
450	9.22×10^{-25}	7.87×10^{-25}	3.99×10^{-24}	3.72×10^{-24}	2.24×10^{-28}	2.24×10^{-28}
500	8.37×10^{-24}	7.25×10^{-24}	3.24×10^{-23}	3.04×10^{-23}	5.11×10^{-27}	5.12×10^{-27}
550	5.18×10^{-23}	4.54×10^{-23}	1.83×10^{-22}	1.73×10^{-22}	6.75×10^{-26}	6.75×10^{-26}
600	2.41×10^{-22}	2.13×10^{-22}	7.90×10^{-22}	7.48×10^{-22}	5.91×10^{-25}	5.90×10^{-25}
700	2.82×10^{-21}	2.53×10^{-21}	8.19×10^{-21}	7.81×10^{-21}	1.86×10^{-23}	1.86×10^{-23}
800	1.87×10^{-20}	1.70×10^{-20}	4.96×10^{-20}	4.76×10^{-20}	2.60×10^{-22}	2.60×10^{-22}
900	8.46×10^{-20}	7.77×10^{-20}	2.10×10^{-19}	2.02×10^{-19}	2.01×10^{-21}	1.87×10^{-21}
1000	2.93×10^{-19}	2.71×10^{-19}	6.87×10^{-19}	6.63×10^{-19}	1.10×10^{-20}	1.03×10^{-20}
1200	2.03×10^{-18}	1.90×10^{-18}	4.38×10^{-18}	4.26×10^{-18}	1.52×10^{-19}	1.44×10^{-19}
1400	8.76×10^{-18}	8.27×10^{-18}	1.78×10^{-17}	1.73×10^{-17}	1.07×10^{-18}	1.02×10^{-18}
1600	2.77×10^{-17}	2.64×10^{-17}	5.37×10^{-17}	5.25×10^{-17}	4.93×10^{-18}	4.71×10^{-18}
1800	7.11×10^{-17}	6.80×10^{-17}	1.33×10^{-16}	1.30×10^{-16}	1.69×10^{-17}	1.62×10^{-17}
2000	1.57×10^{-16}	1.50×10^{-16}	2.84×10^{-16}	2.79×10^{-16}	4.69×10^{-17}	4.52×10^{-17}

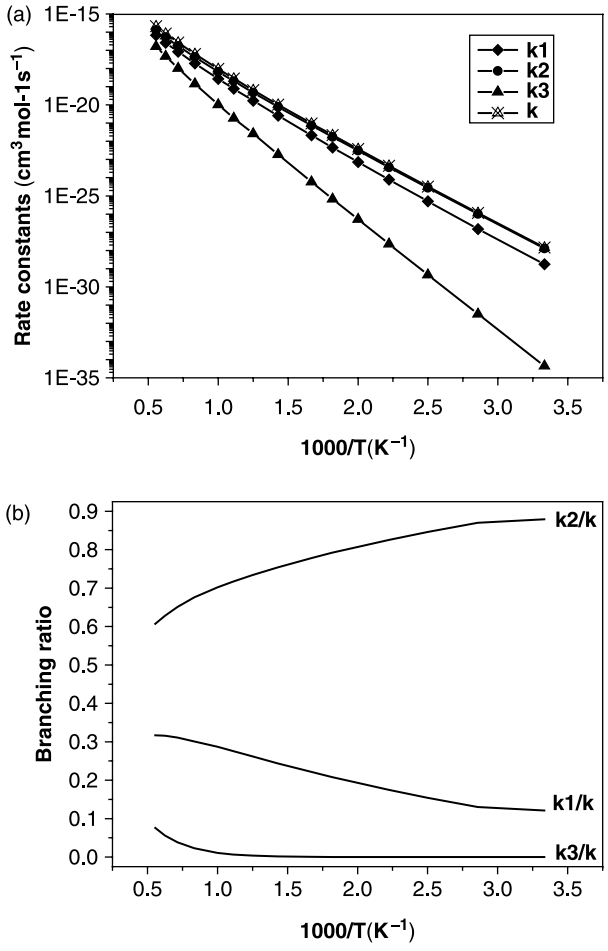

Figure 5. (a) Plot of the calculated individual rate constants *k*1, *k*2, *k*3, and the total rate constants *k* versus 1000/*T* between 300 and 2000 K. (b) Calculated branching ratio versus 1000/*T* between 300 and 2000 K.

3.4 Solvent effects

The synthetic work of organic germanium compounds is usually carried out in solvents. In this paper, the solvent effect is taken into account via the SCRF. SCRF approachs differ in how they define the cavity and the reaction field. We choose the Onsager reaction field model (SCRF = dipole). The solute is assumed to occupy a spherical cavity of radius a_0 in the solvent. The permanent dipole of the solute will induce a dipole (reaction field) in the surrounding medium, which in turn will interact with the molecular dipole leading to stabilisation. In order to obtain more accurate results, we selected the theory level of B3LYP/6-31++G(2d,2p) [18] and the solvent of water.

The total energies, relative energies and dipole moments are shown in Table 4. We compare the stability of the structures in the gas phase and the water solvent, which shows that the polarity of the solvent enhances the stability of structures in the title reaction, and that the dipole moments are increased with the increase in the dielectric constant of the water solvent. As shown in Table 4, in the gas phase, TS1/2b is 4.5284 kJ/mol lower in energy than TS1/2a the title reaction will proceed predominantly via TS1/2b leading to the formation of products. In the solvent of water, TS1/2a is 1.4555 kJ/mol slightly lower in energy than TS1/2b and it was found that the reaction pathway of 1a + 1b → TS1/2a → 2a + 2b is primary for the title reaction in the water solvent. We can also see that the stability of all structures in gas phase is lower than in water solvent.

Table 4. Total energies (E in a.u.), relative energies (E_r in KJ/mol) and dipole moment (Dip in Debye) for all structures at B3LYP/6-31 + +G(2d,2p).

	Structure	Dip	E	E_{rel}
Gas ($\varepsilon = 1$)	$GeCl_3CH_2CH_2COOH$ (1a)	2.5131	−3723.787012	0[a]
	H_2O (1b)	1.9727	−76.44113274	
	TS1/3	4.9371	−3800.185514	111.9259
	TS1/2a	4.2336	−3800.199101	76.2541
	TS1/2b	1.6604	−3800.200826	71.7256
	$GeCl_2OHCH_2CH_2COOH$ (2a)	1.9535	−3339.413741	23.6071[b]
	$GeCl_2OHCH_2CH_2COOH^2$ (3a)	1.0008	−3339.413697	23.7216[c]
	HCl (2b)	1.2309	−460.8054121	
H_2O ($\varepsilon = 78.39$)	$GeCl_3CH_2CH_2COOH$ (1a)	3.0862	−3723.787877	−9.5312
	H_2O (1b)	2.1136	−76.44389747	
	TS1/3	6.5954	−3800.18881	103.2727
	TS1/2a	5.3825	−3800.201779	69.2214
	TS1/2b	2.4264	−3800.201225	70.6769
	$GeCl_2OHCH_2CH_2COOH$ (2a)	2.5981	−3339.414275	19.1411[b]
	$GeCl_2OHCH_2CH_2COOH^2$ (3a)	1.1759	−3339.413641	20.8062[c]
	HCl (2b)	1.413	−760.8065787	

[a] Set the energy of 1a + 1b in gas phase as zero. [b] Relative energy of 2a + 2b. [c] Relative energy of 3a + 2b.

4. Conclusions

In the gas phase, we have thoroughly explored the title reaction by DFT method at B3LYP/6-31++G(2d,2p) level and by the method of the CVT with the SCT effect. The systematic calculations in this study can qualitatively explain the complicated behaviour of the whole reaction. Both the reaction mechanism and the rate constants are reported over the temperature range of 200–2000 K. The dynamic calculations show that the title reaction proceeds dominantly via TS1/2b leading to the formation of products over the whole temperature range in gas phase. Because there are no experimental measurements on the title reaction, some theoretical predictions of rate constants in various temperature may be very useful.

It is noteworthy that the kinetic stability of the three TSs is changed at the B3LYP/6-31++G(2d,2p) level of theory in gas phase and in water solvent. For the two phase of gas and water solvent, the dominating reaction pathway will change from 1a + 1b → TS1/2b → 2a + 2 b to 1a + 1b → TS1/2a → 2a + 2b.

Acknowledgements

The authors thank Professor Donald G. Truhlar for providing the *POLYRATE 9.0* program. This project was supported by the Natural Science Foundation of ShanDong Province (No. Y2003B03, Y2006B42) and the Doctoral Foundation of ShanDong Province (No. 2004BS04011).

References

[1] N. Tanaka et al., *Inhibition of tumor growth and metastasis in association with modification of immune response by novel organic germanium compounds*, J. Biol. Response Mod. 4 (1985), p. 159.

[2] Y. Novik, L.M. Ryan, D.G. Haller, R. Asbury, J.P. Dutcher, and A. Schutt, *Phase II protocol for the evaluation of new treatments in patients with advanced gastric carcinoma: Results of ECOG 5282*. Med. Oncol. 16 (1999), p. 261.

[3] B.J. Kaplan, W. Parish, G.M. Andrus, J.S. Simpson, and C.J. Field, *Germane facts about germanium sesquioxide I. Chemistry and anticancer effects*, J. Altern. Complement Med. 10 (2004), p. 337.

[4] G. Shangguan, F. Xing, X. Qu, J. Mao, D. Zhao X. Zhaob, and J. Rena, *DNA binding specificity and cytotoxicity of novel antitumor agent Ge132 derivatives*, Bioorg. Med. Chem. Lett. 15 (2005), p. 2962.

[5] E.V. Soloviev et al., *Bio-chemical germanium complexes with high therapeutic efficiency and wide application spectrum*, US Patent, No. 6,451,850, 2002.

[6] D.F. Barofsky and E.J. Baum, *Crystal structure of 'carboxyethylgermanium sesquioxide'*, J. Am. Chem. Soc. 98 (1976), p. 8287.

[7] K. Ikemoto, M. Koboyashi, T. Fukumoto, M. Morimatsu, R.B. Pollard, and F. Suzuki, *2-Carboxyethylgermanium sesquioxide, a synthetic organogermanium compound, as an inducer of contrasuppressor T cells*, Experientia 52 (1996), p. 159.

[8] B. Célariès, C. Amourette, C. Lion, and G. Rima, *Germaselenazolidines and germadiselenoacetals: Syntheses and radioprotective properties*, Appl. Organometal. Chem. 18 (2004), p. 684.

[9] C. Lee, W. Yang, and R.G. Parr, *Development of the Colle–Salvetti correlation-energy formula into a functional of the electron density*, Phys. Rev. B Condens Matter. Phys. Rev. B. 37 (1988), p. 785.

[10] J.A. Pople, J.S. Binkley, and R. Seeger, *Closed shell 2nd order Moller-Plesset and MP2 gradient*[*J*], Int. J. Quantum Chem. Symp. 10 (1976), p. 1.

[11] M.W. Wong, M.J. Frisch, and K.B. Wiberg, *Solvent effects. 1. The mediation of electrostatic effects by solvents*, J. Am. Chem. Soc. 113 (1991), p. 4776.

[12] M.J. Frisch, G.W. Trucks, H.B. Schlegel, G.E. Scuseria, M.A. Robb, J.R. Cheeseman, V.G. Zakrzewski, J.A. Montgomery Jr., R.E. Stratmann, J.C. Burant et al., Gaussian03, Revision C.02 Gaussian, Inc., Wallingford, CT, 2004.

[13] J.C. Corchado, Y.-Y. Chuang, P.L. Fast, J. Villa, W.-P. Hu, Y.-P. Liu, G.C. Lynch, K.A. Nguyen, C.F. Jackels, V.S. Melissas et al., POLYRATE version 9.0, University of Minnesota, Minneapolis, 2002.

[14] L. Sheng, Z.-S. Li, J.-Y. Liu, J.-F. Xiao, and C.-C. Sun, Ab initio *direct dynamics studies on the reactions of H atoms with CH_3Cl and CH_3Br*, J. Chem. Phys. 118 (2003), p. 4920.

[15] L. Zhang and Q. Qin, *Computational studies on the reaction pathways of CF_3Br with O(1D,3P) atoms*, J. Phys. Chem. A 105 (2001), p. 215.

[16] T.-J. He, D.-M. Chen, F.-C Liu, and L.-S. Sheng, *The potential energy surface for the decomposition of CH_3OCl*, Chem. Phys. Lett. 332 (2000), p. 545.

[17] Q. Zhang, Y. Gu, and S. Wang, *Theoretical study on the reaction path dynamics and rate constants for the hydrogen-abstraction reaction of atomic O (3P) with CH_2FCl*, Chem. Phys. Lett. 383 (2002), p. 505.

[18] H. Dorsett and A. White, *Overview of molecular modelling and* Ab initio *molecular orbital methods suitable for use with energetic materials*, Published by DSTO Aeronautical and Maritime Research Laboratory (2000).